PHYSICAL REVIEW B

SOLID STATE

THIRD SERIES, VOL. 4, NO. 9 1 NOVEMBER 1971

Magneto-Optical Study of the Spin-Lattice Relaxation of Fe^{3+} in MgO†

Jack C. Cheng and James C. Kemp
Department of Physics, University of Oregon, Eugene, Oregon 97403
(Received 15 January 1971)

A double-resonance method, using the combination of magnetic circular dichroism (MCD) and electron spin resonance (ESR), is used to measure the ratio of the two independent spin-phonon tensor components G_{11} and G_{44}. For Fe^{3+} in MgO, the obtained ratio G_{11}/G_{44} is compared with both the ultrasonic method of Shiren and the static method of Watkins and Feher. An analysis of the double-resonance data indicates that the pattern is extremely sensitive to the form of the spin operator used for the spin-phonon interaction term. It is found that the proposed form gives a good fit to the experimental data. An added feature of the double-resonance method is the ability to correlate directly the optical absorption bands of Fe^{3+} in MgO with its well-known electron spin resonance. It has been found that both the 4.4- and the 5.7-eV charge-transfer optical-absorption bands originate from the Fe^{3+} ground state.

I. INTRODUCTION

Extensive work has been done on the theory of the spin-lattice relaxation mechanism of the S-state paramagnetic ion.[1–3] Experimental results by Watkins and Feher[4] on the uniaxial stress of the Fe^{3+} impurity ions in MgO yield the magnitude and sign of the two independent strain tensors G_{11} and G_{44}. This measurement enabled Sharma[3] to critically test the relative importance of the various spin-lattice mechanisms proposed by Blume and Orbach,[5] Pryce,[6] and others.[7,8] One of the unsettled questions concerning the spin-lattice relaxation mechanism for S-state ions is the relative importance of the covalent properties of the Fe^{3+}:O^{--} complex to the spin-lattice mechanism. Kondo[9] was the first to calculate the spin-lattice relaxation taking covalency of the complex into account, and he found that covalency indeed contributed significantly to the relaxation mechanism. Recently, Sharma[3] also made detailed calculations and his results reversed Kondo's conclusion concerning the importance of covalency.

This uncertainty as to the importance of covalency is due mainly to the lack of experimental data on the location of the charge-transfer bands and their associated charge-transfer parameters.[10] In this paper we identify the two lowest-energy charge-transfer bands associated with the Fe^{3+} impurity ion in a MgO host crystal by the use of a magnetic-circular-dichroism–electron-spin-resonance (MCD–ESR) double-resonance technique. Furthermore, we show that the temperature-dependent part of the MCD can be used to obtain the ratio of the two independent strain tensors G_{11}/G_{44} for the Fe^{3+} ion in MgO. This reflects the MCD–ESR double-resonance signal's dependence on both the detailed forms of the ground-state spin-lattice Hamiltonian and the numerical value of the ratio G_{11}/G_{44} strain tensors.

II. EXPERIMENTAL

The method of double resonance, using a combination of MCD and ESR, has the unique ability of studying the ground-state spin-lattice relaxation mechanism and simultaneously providing information on the nature of the excited states. The basic relationship between the MCD and the spin system of the ground state is that the temperature-dependent part of the MCD is shown experimentally in this case to be proportional to the ground-state expectation of S_z.[11] Therefore, monitoring the MCD is equivalent to monitoring the instantaneous distribution of the ground-state spin population. For the case of Fe^{3+} in MgO, the expectation of the z component of spin is given by

$$\langle S_z \rangle = \tfrac{5}{2} B_{5/2}(g \mu_B H_z/kT) \quad . \tag{1}$$

Therefore, the MCD is related to the Brillouin function $B_{5/2}(g\mu_B H_z/kT)$ as follows:

$$\text{MCD} = \text{const} \times B_{5/2}(g\mu_B H_z/kT) \quad . \tag{2}$$

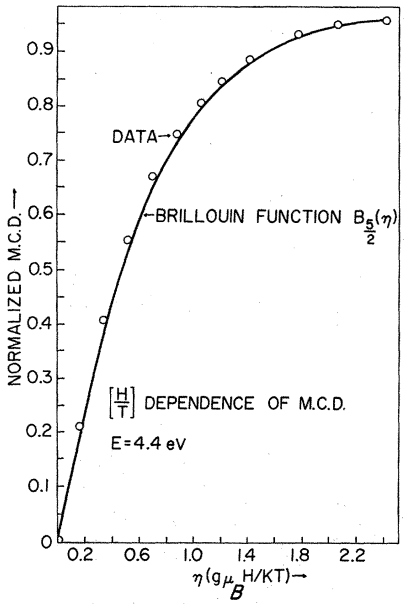

FIG. 1. The normalized MCD dependence of the 4.4-eV optical-absorption band is shown as a function of the ratio H/T. The temperature ranges from 300 down to 1.7 °K, while the magnetic field extends from 0 up to 55 kG.

The experimental data on the temperature and magnetic field dependence of MCD are shown in Fig. 1. The MCD was found to be only a function of the ratio of H_z/T for temperatures ranging from 300 down to 1.7 °K, and magnetic fields extending from 0 up to 56 kG. Since the MCD is proportional to $\langle S_z \rangle$, the application of a strong microwave pumping power would saturate a given set of spin levels, hence changing the $\langle S_z \rangle$ value.

For ions with $S > \frac{1}{2}$, the double-resonance method yields information about the detailed mechanism of spin-lattice relaxation. For Fe^{3+} in MgO the ground state is ${}^6A_{1g}$ and the possible magnetic dipole and quadrupole transitions are shown in Fig.

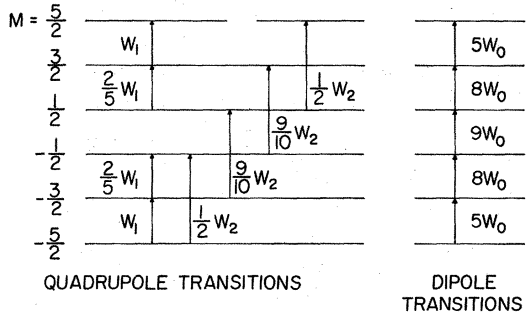

FIG. 2. Two possible types of microwave transitions for the ground state of Fe^{3+} in MgO are shown. In normal ESR experiments, only the dipole transitions are observed.

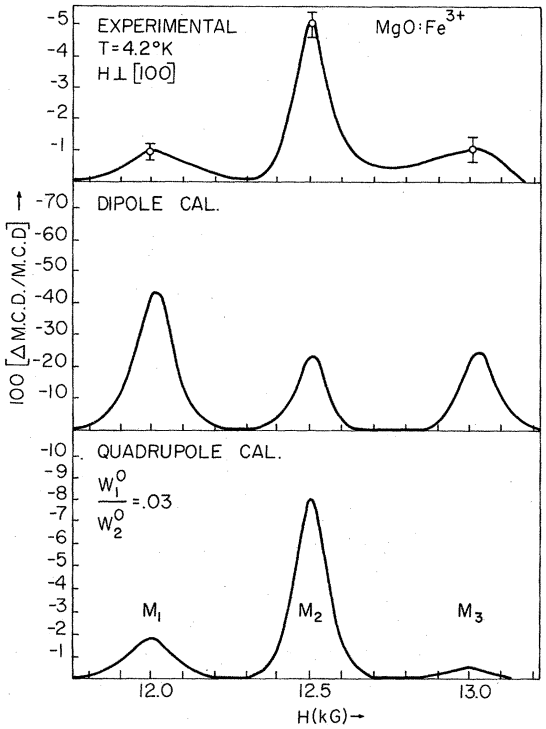

FIG. 3. The experimental double-resonance result is compared with both the dipole and the quadrupole calculations. The calculated quadrupole curve is made to fit the experimental data by having $(M_1/M_2)_{expt} = (M_1/M_2)_{calc}$.

2. It is not clear, without experimental evidence, which process is dominant in producing spin-lattice relaxation. Calculation of the double-resonance pattern indicates that the quadrupole transition is the dominant means of spin-lattice relaxation. The results of the calculation of the double-resonance pattern, along with the experimental results, are given in Fig. 3. It is clear that if the process of relaxation were dipolelike, the shape and magnitude of the double-resonance signal would be quite different. Figure 4 shows the detailed experimental data on the double-resonance pattern and the associated electron-spin-resonance pattern.

To make clear the double-resonance technique which uses a combination of MCD and ESR, an interpretation of the double-resonance pattern shown in Fig. 4 is in order. The crystal of interest, MgO doped with Fe^{3+} ion, is placed in a standard microwave cavity equipped with optical ports, as shown in Fig. 5. The sample is now subjected to two different electromagnetic radiations. The first is the optical electromagnetic radiation (2800-Å light), which is used to obtain the optical MCD signal associated with the optical-absorption band located at 4.4 eV. The pure MCD curve and the associated optical-absorption band are shown in Fig. 6. The second source of radiation is the

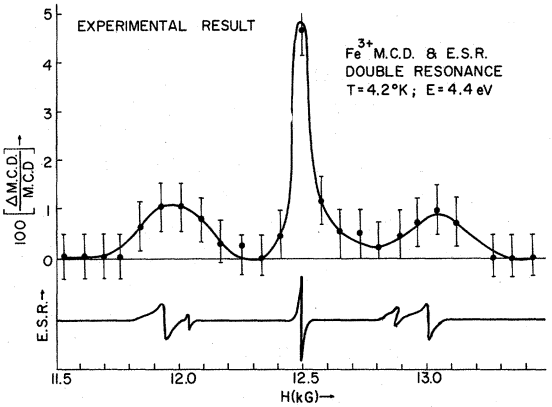

FIG. 4. The detailed experimental double-resonance result of the 4.4-eV band and the associated ESR pattern of the Fe^{3+} ground state are shown. Note the corresponding changes in the double-resonance signal with the ESR signal for a given H field.

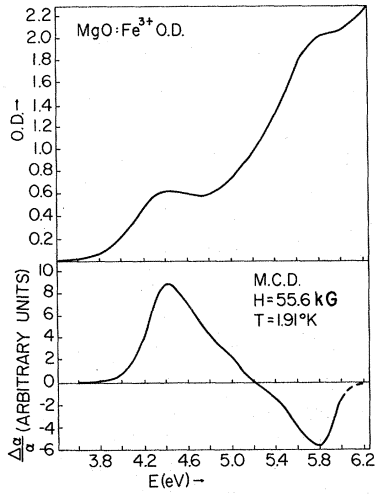

FIG. 6. Both the optical-absorption bands and the MCD are shown as a function of energy in MgO doped with Fe^{3+}. The double-resonance technique demonstrated that both optical-absorption bands situated at 4.4 and 5.7 eV originated from the Fe^{3+} ground states. O.D. stands for optical density.

microwave propagating down the waveguide into the cavity. This microwave power is only absorbed by the Fe^{3+} ions when the ESR resonance condition is satisfied:

$$h\nu\ (\text{microwave}) = g\mu_B H_z \ . \tag{3}$$

The pure-spin-resonance pattern, along with the Zeeman levels involved, is given in Fig. 7. To obtain the double-resonance signal, the optical MCD is monitored at the peak of the MCD band (4.4 eV) and the magnetic field is slowly swept to produce the needed resonance condition. Upon reaching the resonance condition, the spins of the appropriate levels are equalized and so produce a change in the $\langle S_z \rangle$ value. This change is reflected in the decrease of the MCD signal. The normalized change in the MCD along with the ESR patterns are shown in Fig. 4. Notice the corresponding change in the optical MCD when the magnetic field satisfies the ESR resonance conditions.

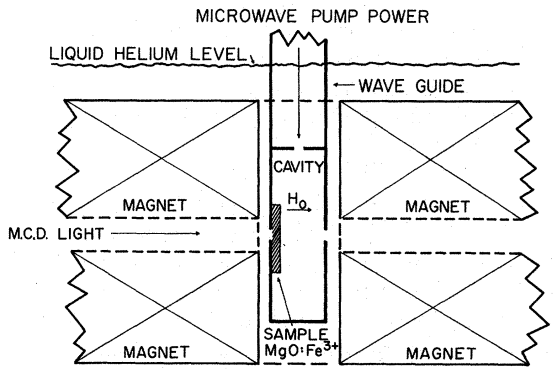

FIG. 5. This is a view of the relative positioning of the various components needed to perform a double-resonance experiment. The graph is not drawn to scale, but rather drawn such that various parts can be shown clearly. The k vector of the light used for MCD is collinear with the external magnetic field produced by the superconducting magnet.

Detailed calculation of the double-resonance pattern is basically a calculation of the change in the $\langle S_z \rangle$ value of the ground state when various levels of the spin-$\frac{5}{2}$ system are saturated by the microwave pumping power. When the magnetic field is applied, the resulting energy levels of the Fe^{3+} ground state in MgO can be described by the following spin Hamiltonian[12]:

$$H_{\text{cub}} = g\mu_B \vec{H}_z \cdot \vec{S} + a\tfrac{1}{6}[S_{x'}^4 + S_{y'}^4 + S_{z'}^4 - \tfrac{1}{5}S(S+1)(3S^2+3S-1)]. \tag{4}$$

In the above expression, x', y', z' refer to the cubic axis of the crystal, while x, y, z refer to the laboratory axis. The g is the spectroscopic-splitting parameter and a is the cubic field-splitting parameter. The ESR signal for the special case in which $x = x'$, $y = y'$, and $z = z'$ is given in Fig. 7, along with the Zeeman splitting of the spin-$\frac{5}{2}$ levels. Fortunately, owing to higher-order interactions involving the spin-orbit coupling and the cubic crystalline fields, [13] the degeneracy of the five ESR transitions is lifted. This lifting enables us to saturate any pair of adjacent levels without directly affecting the others by the microwave. In general, it is possible to have five separate changes of the $\langle S_z \rangle$ value, each associated with one particular ESR line.

In actual experimentation, the changes due to all five ESR lines were not obtained. This is due to

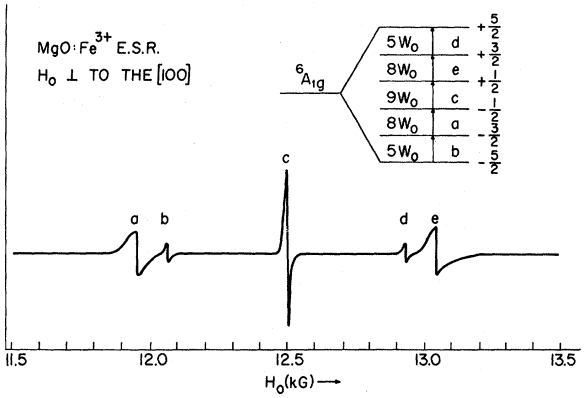

FIG. 7. The ESR signal of MgO : Fe^{3+} is shown along with the Zeeman energy splittings of the Fe^{3+} ground states. The ESR is obtained with the external magnetic field along the [100] crystal direction.

the fact that several of the ESR lines are very close together in this particular orientation of the external magnetic field. When the MCD monitoring system has a relatively long response time, only the resulting average of the two lines can be observed. The double-resonance signal is obtained by slowly sweeping the external magnetic field while monitoring the optical MCD signal. If the magnetic field satisfies the ESR resonance conditions of one particular set of spin levels, the microwave power then saturates that pair of levels and population-equalizes them. When two ESR lines are close together as shown in Fig. 7, and if the time constant of the system is long, it is possible to sweep the H_z field over the two lines in a time which is short compared to the response time of the system. The resulting double-resonance signal is then the averaged effects of the two ESR lines. In particular, if the two lines produce opposite effects on the double-resonance signal, only the net difference is observed. In calculation, unlike the experimental situation, it is possible to obtain the effects of each individual ESR line on the $\langle S_z \rangle$ value. Therefore, to compare the calculation and experimental results, it is necessary to average the effects of those ESR lines which are close together. For example, the ESR transitions labeled a and b in Fig. 7 must be averaged, as must transitions d and e.

The resultant average of the calculated change in MCD consists of three numbers, which represent the normalized change in the MCD as shown in Fig. 3. The first number M_1 represents the net difference between the effects of the ESR transition a and b. The second number M_2 consists of the sole effect of the ESR transition c, and the third number M_3 is again the net difference for the ESR lines d and e. To make the calculated results appear more like the experimental data, three Gaussian curves are drawn in, with the height of the Gaussian curve corresponding to the three numbers and the width corresponding to the experimental width. The results are given in Fig. 3. The width of the Gaussian curve has no real significance, since it represents the response time of the physical measuring system and is a function of the experimental setup. In the limit of fast-response time, the width of the Gaussian curve approaches the intrinsic width of the ESR absorption lines, and the averaging effect for the two adjacent ESR lines also vanishes.

III. THEORETICAL

A phenomenological approach will be used to describe spin-lattice relaxation. The Hamiltonian of the Fe^{3+} ground-state spin system is given in Eq. (8) for the case of a cubic crystalline field. When the cubic symmetry is destroyed by an application of either a noncubic phonon vibration or by external uniaxial stress, an additional term must be added to the spin Hamiltonian. [14] The new spin Hamiltonian describing this system of lower symmetry becomes

$$H = H_{\text{cub}} + H_{\text{ncub}} \quad , \tag{5}$$

$$H_{\text{ncub}} = \vec{S} \cdot D \cdot \vec{S} \quad , \tag{6}$$

where $\vec{S}$ is the spin operator and each component of D is, in general, a linear combination of six strain components[15]:

$$D_j = \sum_i G_{ji} G_i \quad . \tag{7}$$

The constant of proportionality G_{ji} forms the magnetoelastic tensor G. By symmetry arguments, [16] the elements of this tensor can be expressed in terms of only two independent constants: G_{11} and G_{44} for cubic crystals.

According to Kramers's theorem of time reversal, it is clear that the additional term H_{ncub} of the spin Hamiltonian must be even in the spin operator, since otherwise it lifts the degeneracy of the Kramers doublet. The possible form of the noncubic spin Hamiltonian is in general given by

$$H_{\text{ncub}} = H(S^2) + H(S^4) + \cdots \quad . \tag{8}$$

Feher[14] has shown by uniaxial stress experiments on MgO:Fe^{3+} that no contributions from fourth-order terms in the spin variable are necessary in describing the resulting energy levels. This result should be contrasted with the S-state ion of Gd, where the fourth-order terms in the noncubic spin Hamiltonian cannot be neglected. [17] Therefore, keeping only the lowest-order term in the spin variable, H_{ncub} could be written as

$$H_{\text{ncub}} \cong H(S^2) = \vec{S} \cdot D \cdot \vec{S} \quad . \tag{9}$$

Expanding the H_{ncub} Hamiltonian in terms of the strain components, we have two types of transitions

INVESTIGATOR	METHOD	$\left\|\frac{G_{11}}{G_{44}}\right\|$
WATKINS & FEHER	STATIC STRESS	7 ± 15%
SHIREN	ULTRASONIC	5 ± 20%
CHENG	DOUBLE RESONANCE	5.2 ± 20%

FIG. 8. Measured ratio of $|G_{11}/G_{44}|$ for Fe^{3+} ion in MgO.

as given by Shiren[18]:

$$W_1/T = W_1^0[\,|\langle f|S_z S_+ + S_+ S_z|i\rangle|^2] \quad \text{for } \Delta S_z = 1\ , \tag{10}$$

$$W_2/T = W_2^0[\,|\langle f|S_+^2|i\rangle|^2] \quad \text{for } \Delta S_z = 2\ , \tag{11}$$

$$W_1^0 = 6.04\times 10^{-3}\, G_{44}^2\ , \tag{12}$$

$$W_2^0 = 12.08\times 10^{-3}[G_{44}^2 + \tfrac{9}{16}\, G_{11}^2]\ . \tag{13}$$

The above equations are for MgO doped with Fe^{3+} ion having the applied magnetic field parallel to the z crystal axis ($x' = x$, $y' = y$, $z' = z$). We have expressed the transition probabilities W_1 and W_2 at a constant temperature T with the strain tensor components G_{11} and G_{44}. It was found that the ratio $W_1^0/W_2^0 = 0.03$ produces a good fit to the experimental data. From the ratio W_1^0/W_2^0 and using Eqs. (12) and (13), we found the ratio of the G_{11}/G_{44} to be 5.2. The results of Shiren, [18] and Watkins and Feher[4] are given in Fig. 8, for comparison with the result of the double-resonance data.

The actual calculation of the six spin levels's population entails writing down the master rate equations, assuming only the quadrupole mode of relaxation, and solving for the populations of the six levels under dynamic equilibrium[19] ($dn_i/dt = 0$). Since the MCD is proportional to $\langle S_z\rangle$, we have then

$$\Delta(\mathrm{MCD})/\mathrm{MCD} = \Delta\langle S_z\rangle/\langle S_z\rangle\ . \tag{14}$$

The result of a calculation which assumes the dipole transition probability rather than the quadrupole is given in Fig. 3. As can be seen, both the magnitude and shape of the double-resonance curve are different. Because of the large difference in the magnitude of the double-resonance signal between the quadrupole mode versus the dipole mode, this double-resonance method provides conclusive proof of the quadrupole nature of the spin-lattice relaxation process in the ground-state system of Fe^{3+} in MgO.

IV. DISCUSSION

The covalent properties of the Fe^{3+} complex can easily be shown by the observation of several nonforbidden optical-absorption bands. Owing to the difficulties in the oxidation and reduction method employed, early suggestions by Haxby[20] and others[21] to correlate the two optical-absorption bands with the Fe^{3+} impurity were at best plausible. We report here a conclusive identification, using the MCD-ESR double-resonance technique, connecting the ground-state Fe^{3+} ESR with the two charge-transfer bands located at 4.4 and 5.7 eV. As this identification enables us to calculate the oscillator strength of the two charge-transfer bands, we find that for both bands

$$f(4.4\ \mathrm{eV}) \cong f(5.7\ \mathrm{eV}) \cong 0.1\ . \tag{15}$$

Detailed analysis of the MCD data will provide information on the symmetries, degeneracies, and energies of the excited-state charge-transfer wave functions. The experimental MCD data associated with the 4.4- and 5.7-eV optical-absorption bands are shown in Fig. 6. The detailed properties of the charge-transfer bands will be reported upon completion of the theoretical analysis.

ACKNOWLEDGMENTS

Lengthy discussions with Dr. R. M. Mazo during the course of this work are gratefully acknowledged. The author would also like to thank F. A. Modine for aiding in taking part of the experimental data.

†Supported by AFOSR (Solid State Science Division).

[1]R. R. Sharma, T. P. Das, and R. Orbach, Phys. Rev. 149, 257 (1966).

[2]R. R. Sharma, T. P. Das, and R. Orbach, Phys. Rev. 155, 338 (1967).

[3]R. R. Sharma, Phys. Rev. 176, 468 (1968).

[4]G. D. Watkins and E. Feher, Bull. Am. Phys. Soc. 7, 29 (1962).

[5]M. Blume and R. Orbach, Phys. Rev. 127, 1587 (1962).

[6]M. H. Pryce, Phys. Rev. 80, 1107 (1950).

[7]R. Orbach, T. P. Das, and R. R. Sharma, in *Proceedings of the International Conference on Magnetism, Nottingham, England*, 1964 (The Institute of Physics and The Physical Society, London, 1965), p. 330.

[8]H. Watanabe, Progr. Theoret. Phys. (Kyoto) 18, 405 (1957).

[9]J. Kondo, Progr. Theoret. Phys. (Kyoto) 28, 1026 (1962).

[10]Covalency and overlap parameters were obtained in some complexes. See, for example, C. J. Ballhausen, *Introduction to Ligand Field Theory* (McGraw-Hill, New York, 1962), p. 163.

[11]In general, the temperature-dependent part of the MCD is not always a Brillouin function, but rather its functional form depends upon the symmetry of the wave functions involved.

[12]W. Low, Proc. Phys. Soc. (London) B69, 1169 (1956).

[13]W. Low, Phys. Rev. 105, 793 (1957).

[14]E. R. Feher, Phys. Rev. 136, A145 (1964).

[15]W. I. Dobrov and M. E. Browne, in *Paramagnetic*

Resonance, edited by W. Low (Academic, New York, 1963), Vol. II, p. 447.
[16]R. G. Shulman, B. J. Wyluda, and P. W. Anderson, Phys. Rev. 107, 953 (1951).
[17]R. Calvo, R. A. Isaacson, and Z. Sroubek, Phys. Rev. 177, 484 (1969).
[18]N. S. Shiren, in *Proceedings of the Twelfth Colloque Ampère, Eindhoven*, 1962, edited by J. Smidt (Interscience, New York, 1963).
[19]The form of the master rate equations is well known; see, for example, Andrew and Trunstrall, Proc. Phys. Soc. (London) 78, 1 (1961).
[20]B. V. Haxby, Ph. D. thesis (University of Minnesota, 1957) (unpublished).
[21]R. L. Hansler and W. G. Sogelken, J. Phys. Chem. Solids 13, 124 (1960).

PHYSICAL REVIEW B VOLUME 4, NUMBER 9 1 NOVEMBER 1971

Ranges of Recoil Atoms from the (n,γ) Process

William R. Pierson, Joseph T. Kummer, and Wanda Brachaczek
Scientific Research Staff, Ford Motor Company, Dearborn, Michigan 48121
(Received 24 February 1970; revised manuscript received 21 January 1971)

Ranges of ^{198}Au (estimated average energy 50 eV) recoiling from neutron capture in gold film surfaces have been estimated in deuterium, helium, neon, argon, and xenon by measuring the yield on a collector as a function of gas pressure. These ranges are 0.3, 0.54, 1.1, 0.8, and 1.2 μg/cm^2, respectively. From the shape of the curve of recoil yield vs pressure in helium, the range is inferred to be largely independent of energy; this contrasts with the strong dependence known to hold at higher energies. A simple model such as that used for neutron thermalization reproduces the magnitudes and trends of the ranges reasonably well.

INTRODUCTION

The work to be described in this paper deals with ranges of atoms in the 100-eV region of kinetic energy, and with the angular distribution of such atoms when ejected from surfaces. Range measurements in this energy region have not heretofore been attempted, to our knowledge.

An extrapolation of data obtained at higher energies[1–12] suggests that, at 100 eV and less, ranges should be about one interatomic distance. The few indications that actually exist in this energy region are all from (n,γ) recoil studies[13–19] as far as we know, and for the most part these studies indicate that the ranges are of the order of 1 to 10 interatomic distances.

Our method of measurement depends on the fact that an atom recoiling from emission of a γ ray has a kinetic energy

$$E = E_\gamma^2/2Mc^2. \quad (1)$$

(Here, E_γ is the energy of the γ ray, M is the mass of the recoiling atom, and c is the velocity of light.) In the case of neutron-capture γ rays, the recoil kinetic energy is of the order of 100 eV. Recoiling atoms which are ejected from a solid surface are allowed to cross a gas-filled gap to a collector. The number of recoil atoms reaching the collector is measured as a function of gas pressure. With the gap evacuated, a certain number of recoil atoms will reach the collector. As the pressure goes up, more and more atoms are slowed to thermal energy in the gas and diffuse to either the collector or the surface of origin. At sufficiently high pressure, essentially all of the atoms will be thermalized within a short distance and very few will reach the collector. By allowing for diffusion, a projected range can be deduced from such data. Then, with some knowledge of the angular distribution of emitted recoils, the range can be estimated.

The range information obtained in this way is quite crude. First of all, the recoil motion and diffusion are not strictly separable. Second, the recoiling atoms are widely distributed in velocity, both in magnitude and direction. Even so, some interesting trends can be seen despite the limitations.

EXPERIMENTAL METHOD

The atoms used in this study are ^{198}Au ejected from gold surfaces by the process ^{197}Au$(n,\gamma)^{198}$Au; ^{198}Au is a β and γ emitter of 2.7-day half-life, and so the number of recoil atoms reaching the collector can be ascertained by the usual means of counting radioactivity, long after the recoil processes have occurred.

The (n,γ) process on ^{197}Au leads to a level in ^{198}Au at 6.5 MeV.[20] The deexcitation from this level is prompt ($\ll 10^{-6}$ sec) and proceeds to the ground state by a complex decay scheme involving a number of alternate pathways (γ-ray cascades). The path consisting of direct transition to the ground state, with emission of a single γ ray of energy 6.5 MeV, is followed only about 2% of the time; the recoil energy [Eq. (1)] in this case would be 115 eV. The rest of the time the recoil energy